JASA ARTICLE

North Sea soundscapes from a fish perspective: Directional patterns in particle motion and masking potential from anthropogenic noise

Peter Rogers,[1] Elisabeth Debusschere,[2] Dick de Haan,[3] Bruce Martin,[4,a)] and Hans Slabbekoorn[5,b)]
[1]*Georgia Institute of Technology, North Avenue, Atlanta, Georgia 30332, USA*
[2]*InnovOcean Site, Flanders Marine Institute, Wandelaarkaai 7, Ostend, 8400, Belgium*
[3]*Wageningen Marine Research, Haringkade 1, IJmuiden, 1976 CP, The Netherlands*
[4]*JASCO Applied Sciences, Dartmouth, Nova Scotia, Canada*
[5]*Institute of Biology, Leiden University, Sylviusweg 72, Leiden, 2333BE, The Netherlands*

ABSTRACT:
The aquatic world of animals is an acoustic world as sound is the most prominent sensory capacity to extract information about the environment for many aquatic species. Fish can hear particle motion, and a swim bladder potentially adds the additional capacity to sense sound pressure. Combining these capacities allows them to sense direction, distance, spectral content, and detailed temporal patterns. Both sound pressure and particle motion were recorded in a shallow part of the North Sea before and during exposure to a full-scale airgun array from an experimental seismic survey. Distinct amplitude fluctuations and directional patterns in the ambient noise were found to be fluctuating in phase with the tidal cycles and coming from distinct directions. It was speculated that the patterns may be determined by distant sources associated with large rivers and nearby beaches. Sounds of the experimental seismic survey were above the ambient conditions for particle acceleration up to 10 km from the source, at least as detectable for the measurement device, and up to 31 km for the sound pressure. These results and discussion provide a fresh perspective on the auditory world of fishes and a shift in the understanding about potential ranges over which they may have access to biologically relevant cues and be masked by anthropogenic noise.
 https://doi.org/10.1121/10.0006412
(Received 11 November 2020; revised 30 July 2021; accepted 11 August 2021; published online 27 September 2021)
[Editor: Arthur N. Popper] Pages: 2174–2188

I. INTRODUCTION

The aquatic world of animals is an acoustic world, which has been changing rapidly since the industrial revolution (Wenz, 1962; McDonald *et al.*, 2006; Hildebrand, 2009; Frisk, 2012). Biotic and abiotic sounds dominated the acoustic environment in which aquatic animals have evolved, but there is a recent anthropogenic addition of a worldwide rise in shipping traffic and exploitation of marine resources (Sertlek *et al.*, 2019; Miksis-Olds *et al.*, 2018; Duarte *et al.*, 2021). Hearing has evolved in many aquatic animals and typically allows the extraction of information from the surroundings in more detail and at larger distances than with any of the other senses (Au, 1993; Gannon *et al.*, 2005; Simpson *et al.*, 2005; Fay, 2009). Acoustic descriptions of these biologically relevant underwater soundscapes are important because human activities may have such a widespread impact, geographically and taxonomically, that we may speak of acoustic climate change, which should, therefore, be of global concern (Slabbekoorn *et al.*, 2018; Slabbekoorn, 2019; Duarte *et al.*, 2021).

Ambient sounds provide aquatic animals who are capable of hearing them with information about the presence, direction, distance, and movement of their sources (Slabbekoorn and Bouton, 2008; Fay, 2009). Biotic sources are habitat specific and vary with the local and transient animal communities as well as with the season. Abiotic sources include wind, rain, sea state, ice, tidal currents, or turbulence-related bubble formation (Wenz, 1962; Wilson *et al.*, 1985; Prosperetti, 1988). The sounds of localized sources reveal the directions and distances of potential partners, prey items, and predators, or distinct habitat transitions such as reef systems, seagrass or kelp areas, rocky shores, beaches, or estuary entrances (e.g., Radford *et al.*, 2010; Kennedy *et al.*, 2010; McWilliam and Hawkins, 2013). Animals may also perceive the moving position of conspecifics, prey organisms, or calls of approaching predators (Engelmann *et al.*, 2000; Strobel and Mooney, 2012) or localize noisy human activities such as shipping, pile driving, fishing, dredging, sonar, and seismic surveys (Coquereau *et al.*, 2017; Yang *et al.*, 2018; Sertlek *et al.*, 2019).

The presence of noisy human activities may damage, deter, distract, interfere, or just be audible to aquatic animals (Ladich, 2008; Slabbekoorn *et al.*, 2010; Hawkins *et al.*,

a)ORCID: 0000-0002-6681-9129.
b)Electronic mail: h.w.slabbekoorn@biology.leidenuniv.nl

2015; Erbe *et al.*, 2016; Cox *et al.*, 2018; Southall *et al.*, 2019; Popper and Hawkins, 2019). Behavioural and physiological properties can be considered to be the most important as they potentially yield effects at population and, possibly, ecosystem level (Kunc *et al.*, 2016; Soudijn *et al.*, 2020). They have potential impact at moderate levels but over large distances from the noisy human activities, reaching many species and individuals (Slabbekoorn *et al.*, 2010; Popper and Hawkins, 2019). Masking occurs when, for example, sounds from human activities overlap in time, frequency, and direction with biologically relevant sounds (Brumm and Slabbekoorn, 2005; Erbe *et al.*, 2016; Dooling and Leek, 2018). The active range of a signal is determined by the three-dimensional (3-D) space in all directions away from the source over which it is still audible and relates to potential communication distance. Masking issues and active ranges are still relatively unexplored under field conditions and complex to determine as signal detection is dependent on the source level, ambient noise level at potential receivers, as well as propagation conditions (Larsen and Radford, 2018; Brumm and Slabbekoorn, 2005; Erbe *et al.*, 2016; Dooling and Leek, 2018).

Aquatic animals vary dramatically in terms of their spectral hearing capabilities and the aspects of sound they are sensitive to (Southall *et al.*, 2019; Popper and Fay, 2011; Ladich and Fay, 2013; Popper *et al.*, 2014). Marine mammals are sensitive to the pressure aspect of sound, whereas fish and invertebrates are primarily sensitive to the particle motion aspect of sound (Popper and Fay, 2011; Nedelec *et al.*, 2016; Popper and Hawkins, 2018). The integrated processing of both aspects is likely critical for localization and distance assessment in many fish species with a swim bladder (Sand and Karlsen, 1986; Schuijf, 1975; Schuijf and Hawkins, 1983). There is also variety and taxon-specific bias in the acoustic structure of biologically relevant sounds. Many marine mammals generate noisy broadband signals as well as high-frequency, tonal whistle-type sounds that can have harmonics and complex fluctuations. Fish and invertebrates are typically listening for relatively low-frequency, broadband, crackling, clicking, or buzzing sounds with relevant variety in the temporal patterns and spectral composition (Ladich, 2008; Fine and Parmentier, 2015; Amorim *et al.*, 2015).

Very few descriptions of natural or anthropogenically affected underwater sound conditions exist that include particle motion measurements. There are quite a few studies that have reported ambient sound levels with their likely sources (e.g., Wenz, 1962; McCreery *et al.*, 1993; Tolstoy *et al.*, 2004; Estabrook *et al.*, 2016; Erisman and Rowell, 2017; Howe *et al.*, 2019) and community specific patterns, diurnal or seasonal cycles, or habitat-specific spectra (Radford *et al.*, 2010; Kennedy *et al.*, 2010; Staaterman *et al.*, 2013; Lillis and Mooney, 2018; Martin *et al.*, 2019). There are also studies that report audibility ranges for specific biologically relevant sound sources and particular target species (e.g., Radford *et al.*, 2008; Ahonen *et al.*, 2017; Halliday *et al.*, 2018). However, all of these studies addressed primarily just the sound pressure, and although sound pressure is proportional to particle velocity in the far field, it lacks the directionality aspect, and particle motion close to the source, seabed, and sea surface, is often not simply related to the sound pressure (Nedelec *et al.*, 2016; Popper and Hawkins, 2018).

The technology to assess spatial variation and directionality in underwater sound fields is by no means novel. Arrays of multiple sound pressure sensing hydrophones have been used to model the directionality (beam forming) based on correlating the sensor position and variation in sound arrival times (e.g., Cox, 1973; Walker and Buckingham, 2012; Fried *et al.*, 2013; Yang *et al.*, 2018). Also, co-modulation at different frequency bands can be used to deduce spatial information through inference of the source directions and distances from the spectral coherence (Nichols and Sayer, 1977; Nichols and Bradley, 2019; Zhou, 2020). Vector sensors (Wilson *et al.*, 1985; D'Spain *et al.*, 2006; Thode *et al.*, 2019) are probably one of the most informative methods and may match the perceptual world of fishes best (Popper and Fay, 2011; Nedelec *et al.*, 2016; Popper and Hawkins, 2018). The vector sensors obtain directionality by measuring the acoustic particle acceleration along two orthogonal horizontal axes along with the omnidirectional sound pressure and have been applied to the detection and tracking of whales (Thode *et al.*, 2000; Greene *et al.*, 2004). However, as far as we know, vector sensors have not been used in this way for the more general soundscape analyses (Thode *et al.*, 2017; Miksis-Olds *et al.*, 2018; Duarte *et al.*, 2021).

In this study, we investigated the underwater sound conditions through long-term recordings of the sound pressure and particle motion from a moored platform at 30 m depth and 50 km off the Belgian coast in the southern North Sea. We explored the acoustic variation in terms of the level and directionality. We also examined the change in underwater sound conditions during an experimental seismic survey that lasted for 3.5 days. We evaluated the likelihood of possible sources of prominent natural sounds that could be biologically relevant to fishes and other aquatic animals. We also determined the time and scale of the potential masking impact by the seismic survey sound pulses (hereafter referred to as "seismic pulses"). We further characterized the local seismic pulse features from the perspective of the perceptual abilities of fishes.

II. METHODS

A. Site description

We collected our acoustic recordings in Belgian territorial waters in the southern part of the North Sea (51.670°N, 2.802°E). The area is a shallow continental shelf sea with depths of less than 45 m. We deployed the recording equipment in the southwest corner of Belwind wind farm, situated on the Bligh Bank at the marine border between Belgium and the Netherlands (Brabant *et al.*, 2013; Van der Knaap *et al.*, 2021), about 50 km offshore (see Fig. 1). Belwind has

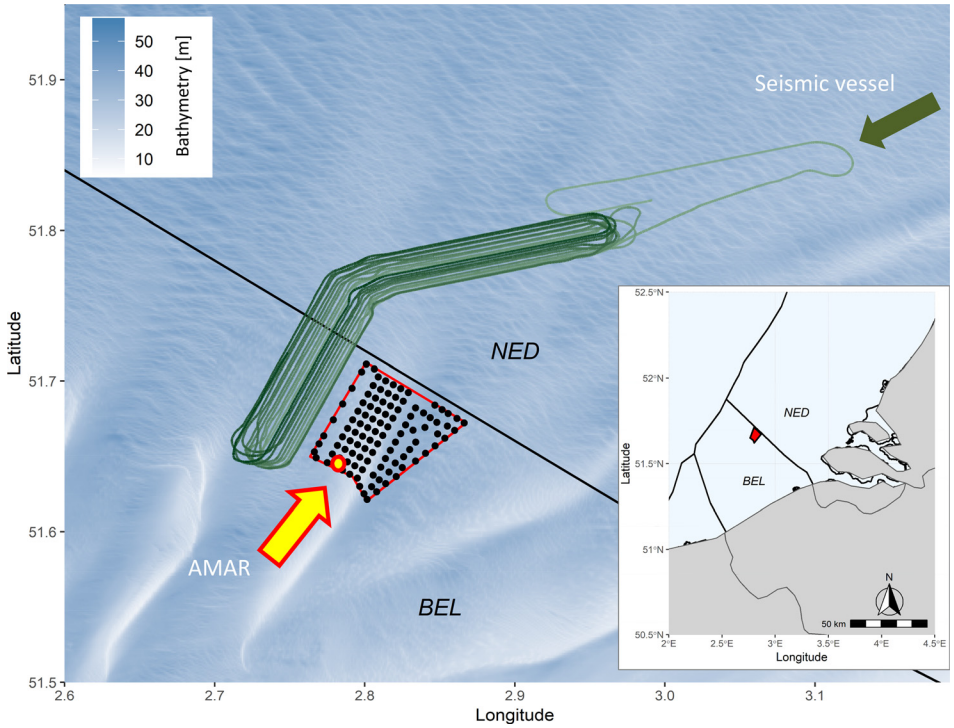

FIG. 1. (Color online) Map of the location of Belwind wind farm (in red; turbines are depicted as black dots) in the Belgian part of the North Sea. The black lines indicate the country borders. The location of the AMAR platform with the recording equipment is at the yellow and red dots with the arrow. The detailed track of the CGG seismic survey vessel MV Geo Caribbean (green line and arrow, line becoming darker in time), starting in the Netherlands, and repeatedly crossing the Dutch-Belgian marine border.

55 turbines with steel monopile foundations; each monopile is surrounded by a protective scour bed of imported basalt or debris stones of various sizes. The monopiles and the scour beds have diameters of 5 m and ~40 m, respectively (Degraer *et al.*, 2019). The seabed between the turbine scour beds is predominantly sand with dunes that may shift position as a result of the tidal currents. The water depth at our study site was between 20 and 30 m, including tidal fluctuations.

B. Experimental seismic survey

An experimental seismic survey was conducted by CGG, Bergen Norway, using the survey vessel "MV GEO Caribbean." The experimental exposure took 82 h in 3.5 days in total, from 20 to 24 July 2018 and was executed to mimic widely used procedures for commercial 3-D seismic survey operations (Gisiner, 2016; Slabbekoorn *et al.*, 2019). The vessel moved at an average speed of 4.8 kn (8.9 km/h), excluding standby and downtime periods. The seismic survey vessel conducted a total of 12 loops and 21 looped transect lines (Fig. 1) with active airguns (accumulating to 52 h) and 41 connecting transition periods (accumulating to 30 h). The first and longest transect line length was 31 km from the north end of the start until the south end of the turn. The average transect line length was 21 km for the series of repeated loops. Scheduled interruptions were restricted to the northern loop ends in the current design to maximize local exposure time for the tagged fish of the experiment (Van der Knaap *et al.*, 2021). There were some additional, short interruptions for operational airgun configuration and necessary performance tests.

The majority of the operation was executed using a primary source array. The first transect line passed Belwind on the west side from north to south with a closest approach distance of 2.25 km to the target site with the tagged fish and our recording devices. The seismic pulse rate was six per minute (10 s intervals), which roughly yielded a pulse at every 25 m. Transect lines were separated by 165 m, on average, moving west from the first track, covering a transect width of about 3 km east-west, and repeating the closest track on the east side two more times. An additional, final, and fourth repeat of the first and closest transect lines were performed using a secondary source array. The primary source array consisted of 36 G-Gun type of airguns, rigged in 3 sub-arrays of 12 cells, and as 6 pairs with equal volume. The full array comprised a total volume of 97 litres (5900 in.^{3}). Each of the airguns was operated for 50% of the total volume at the time and altered for each loop at the northern end of the survey area. At the end of the survey, the secondary source array was operated for 4 h for a single loop. This array consisted of two sub-arrays with a total volume of 48 litres (2930 in.^{3}). Both sources were towed 204 m behind the ship's stern at a depth of 6 m below the water surface with 8 m ±2 m separation between the sub-arrays. For each seismic pulse, the Global Positioning System (GPS) position was recorded with an accuracy of ±1 m.

C. Recording of sound pressure and particle motion

We deployed a lander with recording devices from 13 July to 3 September 2018 in the southwest corner of Belwind wind farm (Fig. 1). The placement was central to the turbines at which cod were caught, tagged, and released (Van der Knaap *et al.*, 2021). Acoustic recordings of the

https://doi.org/10.1121/10.0006412

sound pressure and particle motion were made using a standard omnidirectional hydrophone (M36-V0–100, Geospectrum Technologies Inc., Dartmouth, NS, Canada) along with a three-axis PCB 356B18 MEMS accelerometer (PCB Piezotronics, Depew, NY). The data were recorded with an autonomous multichannel acoustic recorder (AMAR G3), sampling continuously at 32 kHz. The sensors and recorder were mounted on an aluminum plate with the hydrophone ~50 cm above the seabed and ~30 cm above the accelerometers. The accelerometers were fixed inside the AMAR pressure vessel and directly connected to the AMAR endcap, which was rigidly secured to the rectangular bottom plate (55 × 110 cm).

The sensors were selected so that they would accurately record the seismic survey sound levels and directionality while propagating through the water column and substrate. The nominal sensitivity of the hydrophone was −199 dB re 1 V/μPa; when coupled with the AMAR, this yielded a maximum recordable signal level of 202 dB re 1 μPa and a broadband noise floor of ~98 dB re 1 μPa. The hydrophone was calibrated with a pistonphone type 42AC precision sound source (G.R.A.S. Sound and Vibration A/S, ■) before deployment and after retrieval. The manufacturer's calibrations were employed for the accelerometers [nominal sensitivity −139.8 dB re 1 V/(μm/s^2), 0–3000 Hz].

D. Data processing for sound pressure and particle motion

We analysed both natural fluctuations in the ambient noise and anthropogenic fluctuations caused by the seismic pulses. We explored fluctuations in the sound pressure and particle motion for ambient noise patterns during a spring tide (a period of relatively large tidal range, which occurs when the sun and moon are aligned) from 15 to 18 July 2018, early in the recording period, encompassing multiple semidiurnal tidal cycles. We did the same for the seismic exposure period, which happened to be during a neap tide (a period of relatively small tidal range, which occurs when the sun and moon are in quadrature) from 21 to 24 July 2018. The acoustic data were processed for spectral analyses in 83-h blocks, corresponding to the total duration that the seismic source was active. The data were down-sampled to 4 kHz to reduce the storage and computation time while still allowing processing up to 2 kHz, which covers the frequency range relevant to most fish (e.g., Popper and Fay, 2011). The pulse spectra were obtained using the MATLAB PSPECTRUM© m-file (MathWorks, Inc., 2017). The ambient noise for these measurements was estimated from a 30-s time interval when there were no pulses. We investigated the natural soundscape by processing five other 83-h time blocks before and after the seismic source was active, mostly during spring tide intervals where the background sound was the highest. Accelerometer data were converted to particle velocity by numerical integration.

To reliably capture and analyse data from individual seismic pulses, the sound pressure data from the hydrophone were acquired and digitized in 10-s intervals. Because the pulses occurred every 10 s, each interval always includes one seismic pulse. For each interval, the data were circularly shifted to place the maximum peak sound pressure in the centre of the interval. Typically, 20 000 or 29 550 of these 10-s processing intervals are shown in each graph. To further examine the nature of the seismic signal, each 10-s pulse interval was sometimes further subdivided into 20 half-second time bins. Except at the farthest distances, the central bin contained most of the signal energy. For each pulse, the distance from the ship to the receiver was calculated from the ship's GPS, which recorded the position of the ship at each pulse. Corrections were made for the travel time of the signal.

E. Determination of the sound source direction

We determined the direction to a sound's origin for both the natural ambient sound and anthropogenic sound of the seismic pulses. The latter served as a calibration and validation of the azimuth assessment based on the known track for the seismic survey vessel. The directionality can be determined for the dominant sound in a given frequency band. The time average of the acoustic intensity vector $\langle \vec{I} \rangle$ is a non-oscillatory quantity, always pointing directly away from the source of the sound. We obtained $\langle \vec{I} \rangle$ by integrating the product of the pressure and v_y and v_z, obtained from the horizontal components of the tri-axial accelerometer over each 10-s interval. The direction to the source as a function of time was then determined using an arctangent algorithm.

We were able to infer the orientation of the sensor based on the angle to the seismic survey vessel at the closest point of approach (CPA). We measured the direction to the ship at the CPA repeatedly with respect to the accelerometer coordinates. From the ship's GPS track, we could see that the ship was always going in the same direction at the CPA: each time the ship made one of its 11 loops, it passed by another CPA, each time at a different range but always at the same angle. We could also determine the true direction to the ship at the CPA from the GPS track. By subtracting the calculated angle to the ship at the CPA from the true angle, we determined that a 50.17° rotation was required. The graph in Fig. 2 shows good agreement between the corrected angle measure to the ship (indicated by the blue circles in Fig. 2) and GPS-based vessel track, indicated by the red line.

F. Propagation loss and frequency-dependent attenuation

It is important to determine the frequency dependence of the acoustic attenuation between the source location of the seismic pulse and exposure area. Data on the propagation loss will allow the interpretation of likely sources for sounds in the natural patterns of ambient noise and also extrapolation of our data to other areas with known propagation loss. We used the amplitude and spectrum of our acoustic recordings and the GPS-based location of 20 000 consecutive pulses. Because the GPS position of the source vessel and time of each seismic pulse were known, we could determine the distance from the source to the receiver for

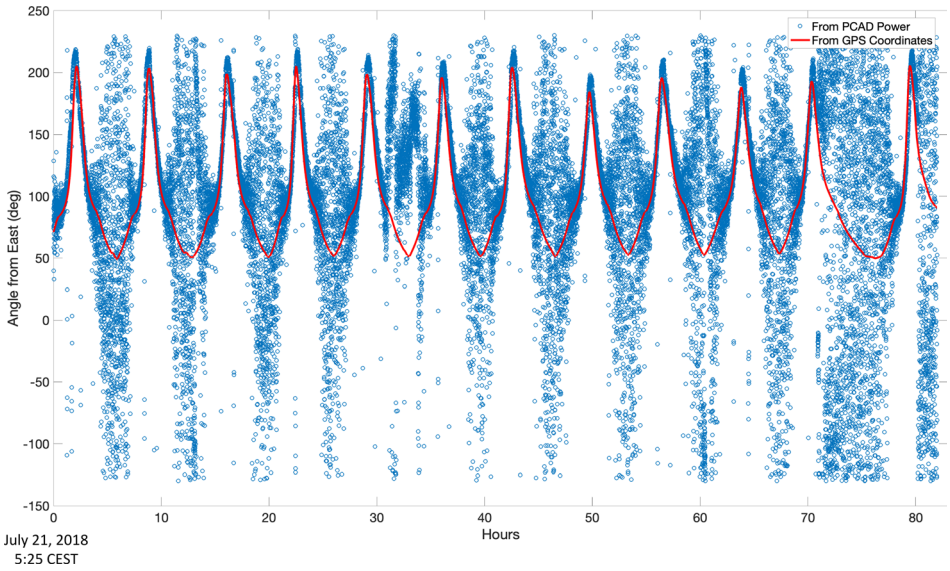

FIG. 2. (Color online) The direction to the sound source of the seismic pulse as computed from the time average of the measured acoustic intensity during the period of the experimental survey (0° is due east; +90° is due south). Each blue point is the calculated angle for a single seismic pulse. The sample points form narrow paths that track the red line of the GPS vessel data precisely. This is especially the case when the vessel is near the closest point of approach (CPA), where the signal-to-noise ratio is the highest, but the track is still visible up to about 4/5 of the maximum seismic vessel distance (which is about 18 km away from the recording device). When the vessel is beyond this distance, the calculated angle becomes more and more scattered, eventually comprising the entire 360° range. There is also evidence for the presence of another boat (other than the seismic vessel) around 30–35 h. Our algorithm tracked the other boat for a while when the source vessel was farthest away and the seismic signal was, therefore, small.

each pulse. Data were obtained for over 10 000 different distances, ranging from 2.25 to about 20 km.

In addition to the location and time, the water depth was recorded for each seismic pulse. Because the vessel trajectory covered most of the propagation paths, the water depths were well sampled. The mean value of the water depth was 35.1 m with a standard deviation of 2.4 m. Some of the depth variance is attributable to the bathymetry and some is due to tides because the measurements occurred over many tidal cycles. The tidal elevations ranged from −1.3 m to +1.3 m (tidal data were obtained from the Royal Belgium Institute of Natural Science[1]). Because all of the propagation distances were much greater than the water depth, there is always cylindrical spreading present, in addition to true attenuation, caused by the surface and seabed interaction. We, therefore, removed the spreading effect by multiplying the acoustic pressure by the square root of the distance to determine the magnitude of this true attenuation with the distance.

G. Ethical statements

We received permission to conduct the experimental seismic survey from both the Belgian authorities [Belgian Department of Bestrijding van de Sociale Fraude, Privacy en Noordzee (BPN) after positive advice from Royal Belgian Institute of Natural Sciences (RBINS)] and the Dutch authorities (MINEZ after positive advice from RWS). The ethical approval for working with live fish, associated with the current study but reported elsewhere (Van der Knaap *et al.*, 2021), was given through Certificate No. EC2017–080, in line with official guidelines for animal welfare in Flanders, and through Permit No. AVD1060020171085 of the Dutch Central Commission on Animal Experiments (CCD), in line with the Dutch Experiments on Animals Act. Furthermore, the experimental seismic survey operation was executed according to the Joint Nature Conservation Committee (JNCC) mitigation measures as well as additional guidelines of the Belgian and Dutch authorities.

The seismic survey transect area was adapted to have the lowest possible impact to Belgian and Dutch Natura 2000 sites. A dedicated and independent marine mammal observer (MMO) was on board throughout the operation and on duty throughout the survey during daylight hours. The MMO night operations were covered by a passive acoustic monitoring system, recruited by the operator CGG. The MMO was assisted throughout the survey period by biologist D.d.H. Sightings of marine mammals within the JNNC defined range (500 m) did not occur, but two shutdowns were executed before entering the Dutch Marine Protected Area exclusion zone "Vlakte van de Raan." At the start of the experimental survey and whenever the airgun array had been passive for more than 10 min, a 30-min marine mammal observation time was taken into account. This was done to exclude the possibility of nearby animals before the source gradually increased to full power in incremental stages over a period of 20–40 min (i.e., "soft-start").

III. RESULTS

A. Amplitude fluctuations and directionality in ambient noise

Both sound pressure and particle motion exhibited distinct fluctuations in the amplitude, synchronized with the

https://doi.org/10.1121/10.0006412

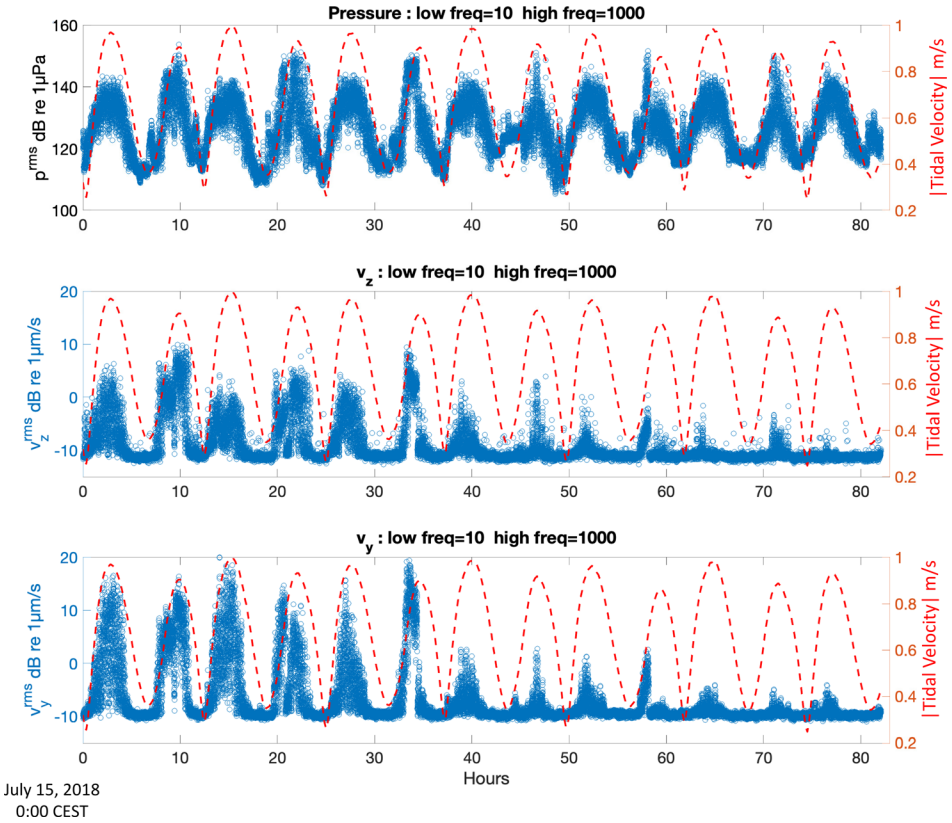

FIG. 3. (Color online) The tidal cycles in (A) sound pressure (rms) and (B) particle velocity (rms) in two horizontal directions, all for the frequency range of 10–1000 Hz. Each data point represents the rms value for 10 s of data. The red dashed lines indicate the local tidal velocity amplitude (m/s) in all three panels, reflecting the tidal fluctuations. The data are taken in the spring tide period from 15 to 18 July 2018 and reveal synchronous amplitude fluctuations in pressure and particle motion at a rate of two peaks per tidal cycle, which are likely associated with the current fluctuations at a distant source. After about 40 h, a significant drop in the particle velocity is visible, independent from the pressure, which is due to an artefact or fading error of the accelerometer channels but which does not affect our directionality measurements. For the absolute levels, we can still rely on the sound pressure measurements as the ratio between the pressure and motion is constant, ρc, for measurements in the far field of a sound source.

rhythm of the tides (Fig. 3). Peaks in the root-mean-square (rms) pressure occurred at six-hour intervals, correlating with the rate of two flow peaks per tidal cycle of roughly 12 h. The pressure waveforms correlated closely with both horizontal components of the particle velocity, indicating that the sound was not originating from a nearby source but coming from far away. Note that at 35 h into the 83 h of the spring tide period shown in Fig. 3, both components of the rms horizontal particle velocity decreased significantly, whereas the rms pressure did not. It appears that the accelerometer channels were fading, and we do not have an explanation. Fortunately, the calibration of the accelerometer does not affect the data on the directionality to the source. Moreover, because the sound pressure and particle velocity are well correlated, the absolute level of the particle velocity can be adequately approximated by dividing the measured sound pressure by the far-field impedance, ρc.

We used the $\langle \vec{I} \rangle$ algorithm, validated for accurate azimuth localization by tracking the angle to the source ship, to determine the direction to the source of the strongest signal detected for each of 29 550 separately processed 10-s intervals with a 9–40 Hz filter in 83 h of ambient noise. The 9–40 Hz band was chosen because it was the band where the noise was the strongest. Distinct and more-or-less persistent directions became apparent as dominant angles of the sound arrival during the low tides under spring tide conditions [Fig. 4(A)]. For example, during the third low tide, the strongest signal was coming predominantly from near −19° for the first 400 intervals, then it alternated between −19° and 161° from intervals 400 to 600, and ending up with the strongest signal coming from a broader region near +19° for the remaining 200 intervals. At the bottom of Fig. 4(A), the results from all six low tides are combined in a single histogram, indicating that there are three dominant directions. The results obtained by repeating the procedure for five separate bands are shown in Fig. 5. The cumulative histograms for the 9–40 Hz band, 10–20 Hz band are nearly identical (and similar to the 10–1000 Hz band), indicating that the directional data were dominated by the 10–20 Hz band. At low tides, for frequencies between 10 and 20 Hz, the sound appeared to originate from within a few degrees of the mouths of the three largest nearby rivers in Belgium, the Netherlands, and the United Kingdom: the Scheldt, the Rhine, and the Thames, respectively (as shown in Fig. 5). For frequencies between 20 and 40 Hz, the pattern had a peak only in the direction of the Rhine, for frequencies of 40–80 Hz, the pattern showed peaks toward both the Rhine and the Thames, and for frequencies of 80–160 Hz, the pattern was just toward the Thames.

The results for the high tides are different: for the 10–20 Hz band, there was just a single very broad peak centred around 50°, which matches the closest beaches around Zeebrugge. For the 20–40 Hz band, the directionality pointed at the Thames again and the North Sea Canal, the waterway from Amsterdam to the North Sea. For the 40–80 Hz band and 80–160 Hz band, there was just a broad peak directed toward the Thames. The data, therefore, revealed distinct patterns of directionality for low and high tides and different low-frequency ranges. The sound pressure amplitude levels also varied between the low and high

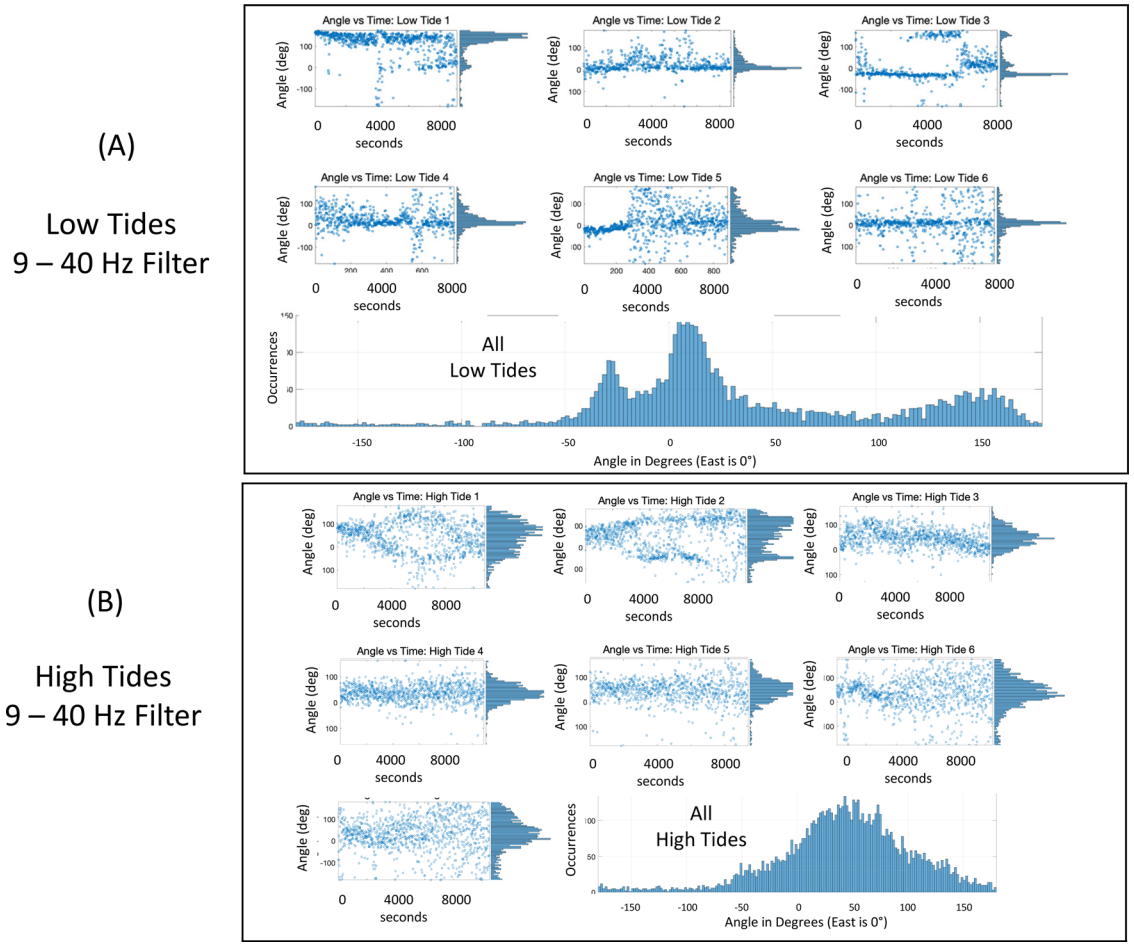

FIG. 4. (Color online) The variation in the dominant direction of the horizontal integrated intensity (bearing to the source) during low tides (A) and high tides (B) in the period of 15 to 18 July 2018 (spring tide period, which included six low tides and seven high tides). The data were filtered from 9 to 40 Hz, which was the band where the noise was the strongest [see Fig. 6(A)]. (A) The detailed information on the dominant directionality of the horizontal intensity over time for each of six low tide periods. Each dot on the scatterplot represents a single 10-s time period. The arrival time associated with each 10-s interval is on the x axis, and the angle to the strongest source detected during the interval is on the y axis. Here, 0° is east and −90° is south. The histogram on the right of each plot accumulates the dominant angles. Also shown is a cumulative histogram depicting the dominant direction-to-source, incorporating all data points from the above six plots for individual low tides. (B) The same as in (A) but for the seven high tide periods.

tides with a different bias across frequencies with higher levels at low tides in the low frequencies around 18 Hz and higher levels at high tides above 80 Hz [Fig. 6(A)]. Ambient neap-tide conditions (high and low tides combined) were 40–50 dB lower than the spring tide conditions in the very low frequencies (<40 Hz) and still 20–30 dB lower at higher frequencies [Fig. 6(B)].

B. Acoustic conditions during the experimental seismic survey

The amplitude levels averaged across the whole seismic survey period (a neap tide) were similar to the ambient spring tide levels in the low frequencies but considerably higher than the ambient conditions for frequencies above 40 Hz (Fig. 6). The anthropogenic sound exposure elevated the neap-tide sound levels by about 50 dB for most of the spectrum, relevant to marine fishes [Fig. 6(B)]. Inspection of the seismic pulse waveforms at different distances revealed a short and sharp, broadband pulse at close ranges. A clear low-frequency precursor wave and low-frequency reverberations became more prominent with distance (Fig. 7). As a consequence, the pulse amplitudes decreased, whereas the pulse duration increased as the ranges increased. The growth of the tail is the result of both dispersion and reverberation. By examining the advance of the precursor relative to the main arrival, we determined that the velocity of the lowest propagating frequency is approximately equal to the speed of sound in the sediment.

Seismic pulses were noticeable above the background sound pressure level (SPL) up to the maximum distance of 31 km. Figure 8(A) shows the decay in time of the seismic pulse relative to the ambient sound level in the frequency range of 40–500 Hz, the presumptive hearing range of the cod. The signal fading increased with increasing distance to the airgun array. The presence of the operational seismic survey vessel elevated the ambient sound levels beyond a range of 21 km for the whole time, including the pulse intervals. This is not the case for particle velocity [in the horizontal direction; Fig. 8(B)]. The pulse of particle velocity in the frequency range of 40–500 Hz is clearly visible at close

https://doi.org/10.1121/10.0006412

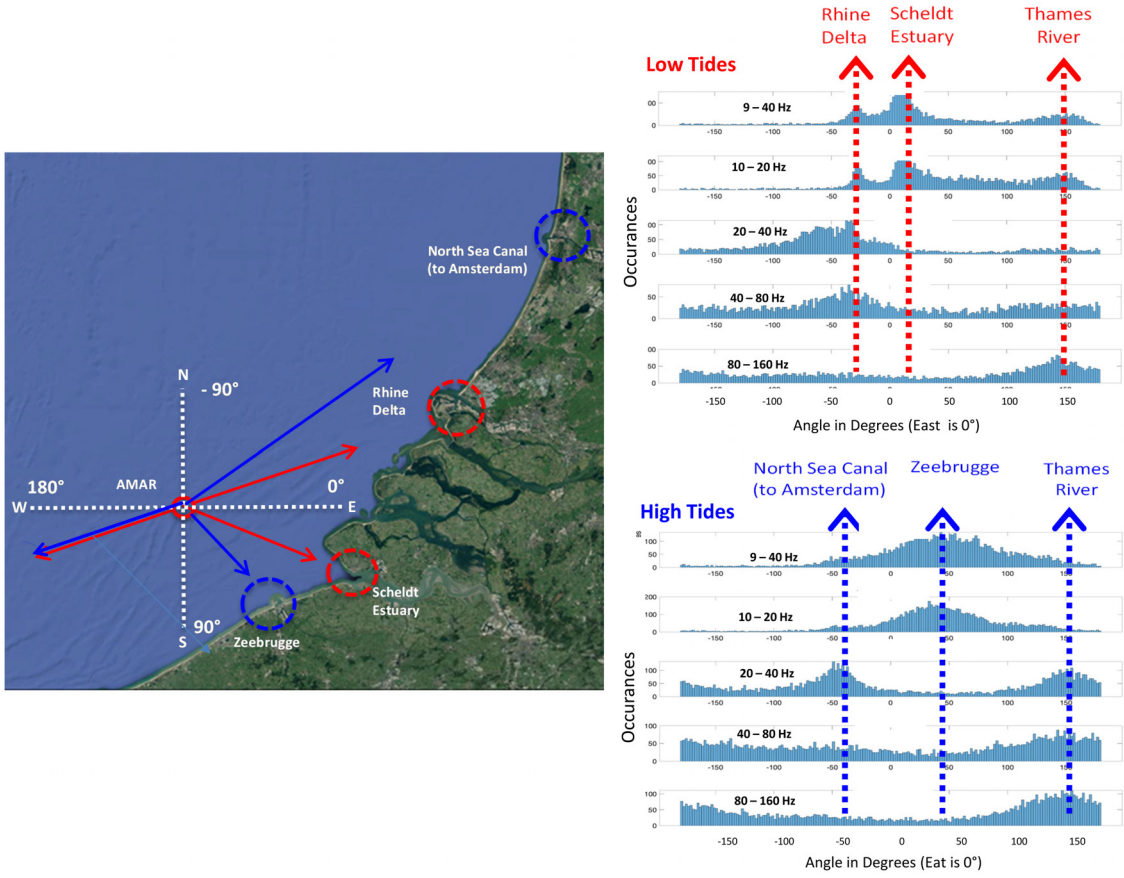

FIG. 5. (Color online) The calculated directions to the sources of the measured ambient noise amplitude peaks for both high tides and low tides during the target spring tide period. (Left) Map of the Belgian and Dutch coast with arrows pointing from the location of the AMAR to the most prominent source directions during high (blue) and low (red) tides with likely source locations at the coastline. (Right) Cumulative histograms for the source directions, calculated from the time averaged intensity levels, with the data filtered in five different, dominant frequency bands (9–40 Hz, 10–20 Hz, 20–40 Hz, 40–80 Hz, and 80–160 Hz), accumulated for the six high and seven low tide periods. The dashed arrows correspond with the directions shown on the map.

range but drops below the ambient noise (or, more likely, the sensor noise floor) when the source vessel is at about 10 km distance. The sounds from the precursor waves and reverberations are only above the ambient noise (or the sensor noise floor) at very close range and just in the 10 s bins directly prior to and immediately after the pulse.

C. Propagation loss and frequency-dependent attenuation

We determined the frequency-dependent attenuation from the seismic pulse recordings with the source vessel at known distances for 20 000 pulses. We conducted a simple linear regression model with distance from the seismic array as the predictor and the SPL as the response parameter for each frequency. It is evident from the data (e.g., Fig. 7) that at frequencies above 100 Hz, the sound pressure fell below the noise floor around 10 km; hence, we terminated the regression at that distance for higher frequencies [Fig. 9(A)]. The quadratic and multivariate models, using tidal height as a predictor, did not improve the fit. The angle between the vessel trajectory and propagation direction was also tried as a predictor but to no avail. This indicated that the airgun array had little or no directivity in the horizontal plane. Based on the size of the array and gun spacing, this would be expected below 40 Hz but would not have been expected at 100 Hz and above.

The attenuation (dB/km) increased with the increasing frequency [Fig. 9(A)]. Note the very low attenuation (less than 1.5 dB/km) at the lowest frequencies, where they would be expected to be very high as the result of a shallow-water cutoff. We compared the attenuation values from the linear regressions across the frequency with values predicted from a simple Pekeris model (Pekeris, 1948). The measured attenuation was much smaller than the predicted attenuation at low frequencies and much larger than predicted at high frequencies [Fig. 9(B)]. The observed low attenuation at low frequencies may be due to a relatively fast reflective layer within the substrate. Deep-diving rays as the cause can be ruled out because the precursors appear to be propagating at the speed of sound in the bottom sediment. The attenuation at high frequencies is likely caused by roughness at various interfaces, including surface and scour bed roughness, and possibly related to the prominent undersea sand dunes.

IV. DISCUSSION

We found distinct fluctuations in the sound pressure and particle motion levels in the natural ambient noise patterns in the shallow, southern part of the North Sea. Acoustic

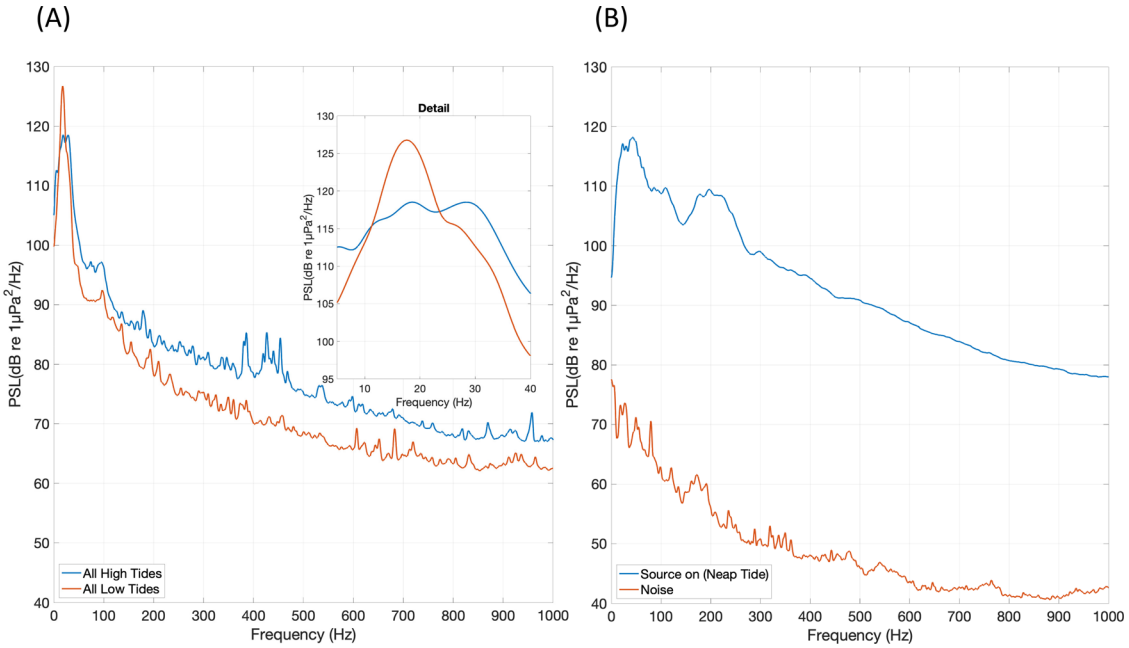

FIG. 6. (Color online) The spectral composition of both the natural ambient noise spectra and cumulative anthropogenic noise spectrum of the experimental seismic survey sound exposure. (A) The pressure spectral density for ambient spring tide sound conditions for all low tides (red) and all high tides (blue). (B) The pressure spectral density for sound conditions during the entire seismic survey (blue line) and a representative 300-s sample of ambient neap-tide conditions without the seismic sound pulses.

fluctuations occurred in synchrony with the tidal currents. The sound intensity data revealed variable patterns of directional dominance, horizontally pointing into directions of possible long-distance sound sources, such as coastal surf and tidal river currents. Seismic pulses degraded with distance with low-frequency precursors and reverberations filling the pulse intervals. The pulse signal was above the ambient up to 21–31 km, depending on the strenth of the tides for the sound pressure, and up to 10 km for the particle motion as measured by our device. We found unexpected sound propagation conditions in the attenuation, which were much lower than expected for the lowest frequencies and higher than expected for the higher frequencies.

A. Alternative explanations for natural soundscape patterns

Natural peaks in the SPL during the target spring tide period occurred at 6-h intervals, correlating with the typical rate of two tide-associated currents. There was considerable and consistent variation in the amplitude patterns over time, the energy bias across the spectra, but especially in the directional patterns between the low and high tides. This combined acoustic picture strongly suggests that multiple and separate sound sources are responsible for these complex patterns. The synchrony of the amplitude fluctuations with the tidal cycle makes current-related turbulence and sound generation a likely candidate as possible sound sources.

However, the current-related sound generation could take place at various distances and could be due to (1) an artefact of flow noise directly around the lander or recording equipment; (2) strong currents around turbines or boulders in the scour bed at tens or hundreds of meters; or (3) loud sources at more distant locations, kilometres to tens of kilometres away. The measured pressure correlated well with both horizontal components of the particle velocity, which is not expected from a source in the near field (Urick, 1975; Jensen, 2011), and indicated that the sound was coming from beyond the direct vicinity of our equipment. The closest turbines were all further than 150 m away and, thus, beyond the near field for sounds in the range of 10–40 Hz. However, the four nearest turbines were at angles of 140° (B10), −50° (C09), −95° (B10), and 80° (C10), which do not match with the observed directional patterns. Moreover, the principal difference between the flow at low and high tides is a reversal in the direction of flow, which would not explain the spectral or directional variations in the observed sounds.

We believe that the most likely current-related sound sources that could be responsible for the amplitude fluctuations and distinct directional patterns in the two low-frequency bands of 10–20 Hz and 20–40 Hz are river mouths from some of the main Belgian, Dutch, and English rivers (Scheldt Estuary, Rhine Delta, North Sea Canal, and Thames River). Although the details of the temporal match with fluctuations in the tidal currents at distant sites should be tested, the geographical match is quite compelling for the directional sound data with the constellation of large rivers. The major estuaries are expected to have tide-related water turbulence, which would also be distinct for low and high tides (flowing with and against the river stream). The sounds potentially associated with river sources dominated primarily at low tide when the tidal currents are usually the highest. Although turbulence *per se* is a quadrupole source and, thus, does not radiate strongly to the far field, the presence

https://doi.org/10.1121/10.0006412

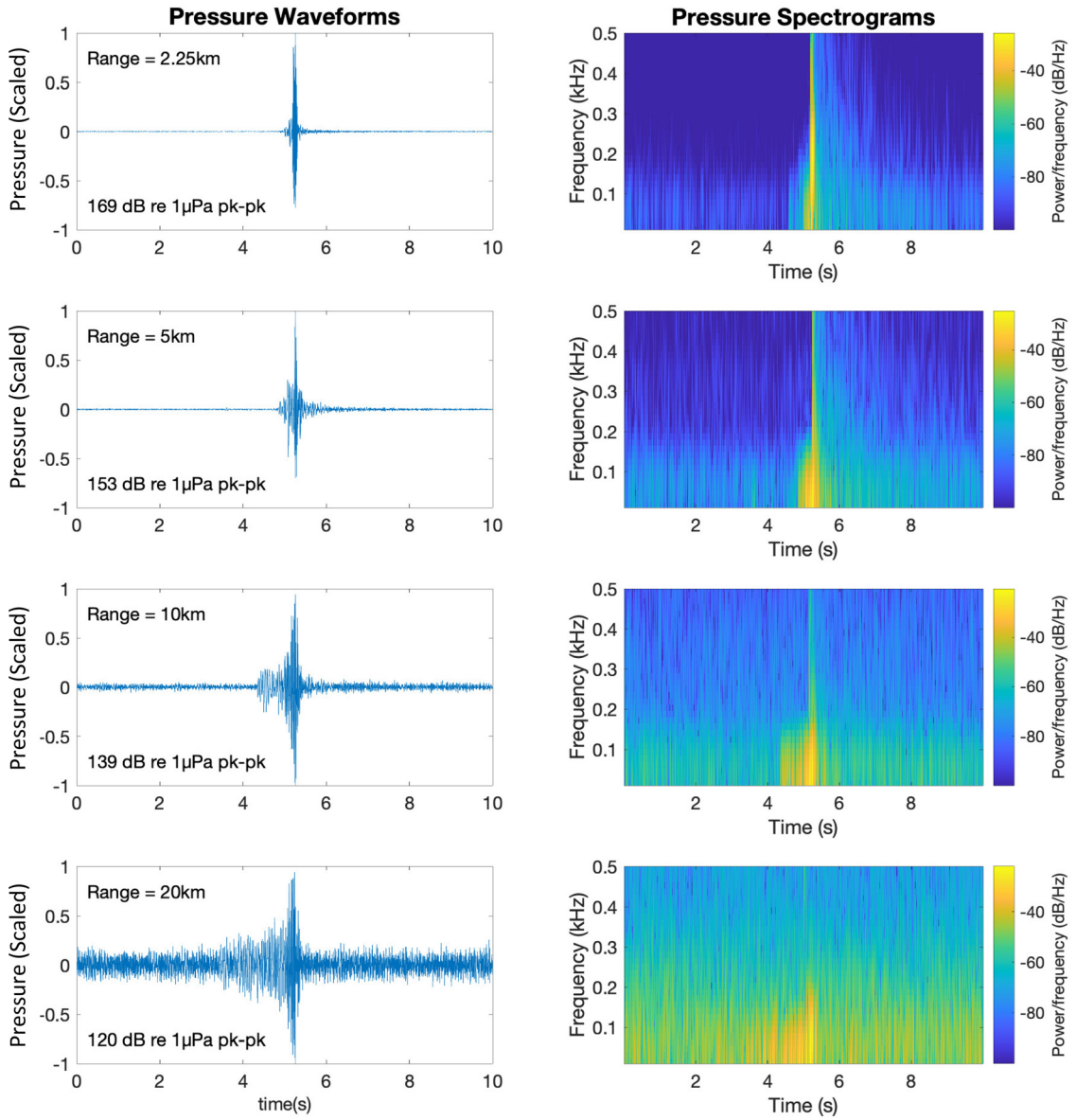

FIG. 7. (Color online) The representative seismic survey sound pressure waveforms (left) and corresponding spectrograms (right) at 2.25 km (CPA), 5 km, 10 km, and 20 km. The waveforms illustrate the growing presence with the distance of the precursor wave before the pulse and growing presence with the distance of reverberations after the pulse. The spectrograms show the broadband features of the pulse and the lower frequency nature of both the precursor and reverberations.

of bubbles can transform the quadrupole radiators into strongly radiating monopoles (Crighton, 1975).

Surf noise from the nearby sandy shores of Belgium likely also contributed to the patterns in the directionality data. Surf noise should yield directional sound from a smear of points along the line source of the nearest beaches around Zeebrugge. The directional pattern from the Belgian beaches appears to become dominant for high tide as would be expected from surf noise. The interpretation of our directionality data, which is being caused by the tidal cycles in distant sources at major river mouths and nearby coastline, is still a hypothesis that requires further testing.

B. Discarding some more alternative sound sources

Distant shipping is a significant factor in many oceans and seas (Zhou, 2020), including the North Sea (Sertlek *et al.*, 2019). The nearby Scheldt Estuary with the Western Scheldt serving Antwerp harbour and the Rhine Delta, serving Rotterdam harbour, would also make shipping noise a possible factor. The dominance of the 10–40 Hz in the directional pattern could also be expected as the presence of sound energy attributed to shipping gradually declines with the increasing frequency (Sertlek *et al.*, 2019), and we determined the local attenuation profiles with relatively good low-frequency propagation. However, the shipping lanes from the Western Scheldt would likely not yield very localized azimuth patterns but very broad smears as boats pass by in the northeast at angles from the southeast (30°) to the north (−90°) and in the south, at angles from the southeast (30°) to the southwest (150°; Nilsson *et al.*, 2017). Furthermore, the distinct patterns in the different frequency bands of 10–20 Hz and 20–40 Hz are not expected from shipping and

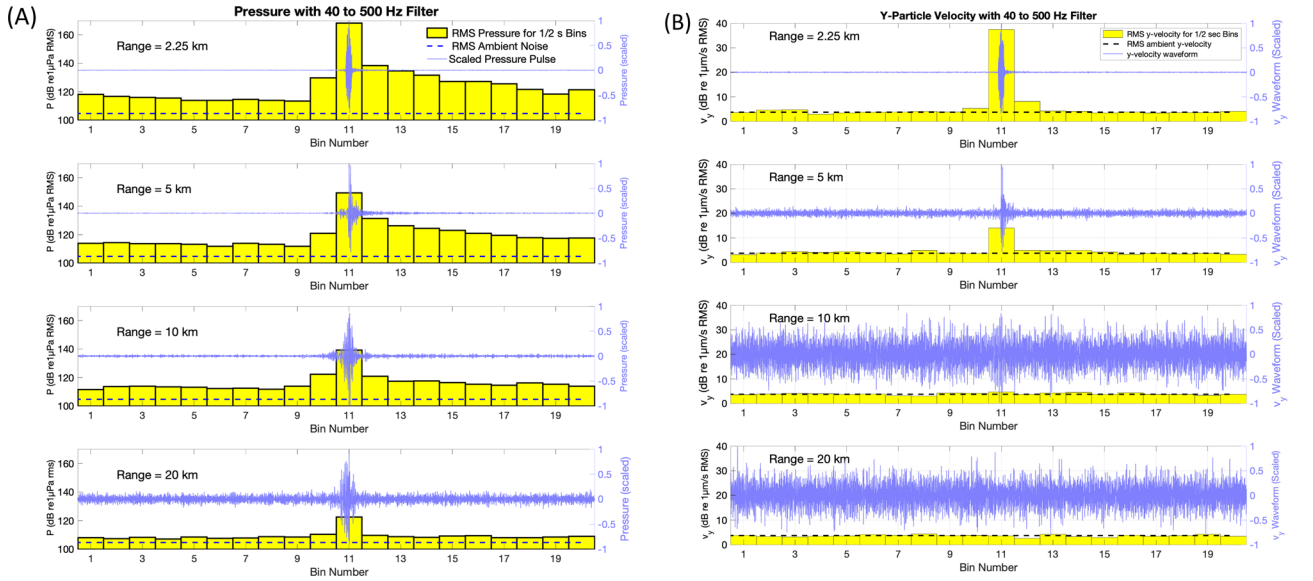

FIG. 8. (Color online) The signal and noise sound pressure and particle motion at four different distances during and in between seismic pulse sounds. rms values for 0.5-s time bins for (A) pressure and (B) the larger component of the horizontal particle velocity. The yellow bars show the result of subdividing each 10-s pulse period into 20 half-second bins, circularly shifting them such that the main pulse is located in bin 11. The height of the bar corresponds to the rms pressure or particle velocity of the sound within the time bin. The scaled waveform is shown as the reference in time. The dashed horizontal lines indicate the ambient noise level. The data were filtered from 40 to 500 Hz to approximate the frequency range of the acoustic sensitivity for Atlantic cod (and many other marine fishes).

neither is the correlation of the amplitude fluctuations with the tidal cycles.

The local sea state-related wave noise (Longuet-Higgins, 1950; Wenz, 1962; Duennebier *et al.*, 2012) is also not expected to explain the patterns in the directionality. The prominence and variance in terms of the synchrony with the tides would not be expected, and the bias in our data to low frequencies does not match well. Wave noise may also generate low-frequency sound up to 80 Hz, but wind-induced noise is typically gradually increasing in prominence toward 1 kHz and is most prominent between 1 and 10 kHz (Sertlek *et al.*, 2019). The swell from distant storms can be highly directional (Wilson *et al.*, 1985; Zhou, 2020) but would be expected to follow the main possible arrival trajectories from the north (northern parts of the North Sea) or southwest from the English Channel, which is again not reflecting the data.

C. Seismic survey exposure conditions and potential consequences

There are many studies showing the behavioural or physiological effects from sound exposure on fishes (Slabbekoorn *et al.*, 2010; Cox *et al.*, 2018; Popper and Hawkins, 2019), but assessing impact on free-ranging individuals from an anthropogenic source, such as a seismic survey, remains difficult and rarely performed (Pearson *et al.*, 1992; Hassel *et al.*, 2004; Fewtrell and McCauley, 2012; Bruce *et al.*, 2018; Carroll *et al.*, 2017; Morris *et al.*, 2018; Morris *et al.*, 2020; Slabbekoorn *et al.*, 2019; Kok *et al.*, 2021). The sounds from anthropogenic activities may reach fish by direct propagation through the water column or indirect propagation through the substrate (Hazelwood, 2012; Roberts and Elliot, 2017; Popper and Hawkins, 2019). Detailed behavioural response data may provide insight into the energy budget changes related to increased swimming activities or decreased foraging efficiency (Davidsen *et al.*, 2019; Hubert *et al.*, 2020), which may be translated to population level consequences (Kunc *et al.*, 2016; Slabbekoorn *et al.*, 2019; Soudijn *et al.*, 2020).

Van der Knaap *et al.* (2021) studied the responses of tagged cod before, during, and after the exposure conditions described here for the experimental survey (also see Kok *et al.*, 2021 for an echosounder view on pelagic fishes during the same survey). The free-ranging cod did not leave the area during the exposure but appeared to have a delayed response with a significantly elevated probability to leave afterward. Van der Knaap *et al.* (2021) also found behavioural effects for the fish that stayed during the seismic survey as these individuals spent significantly less time being locally active (likely including foraging behaviour) and switched to being more inactive. Although Van der Knaap *et al.* (2021) did not find a clear dose-response pattern, they did reveal that the daily rhythm of the cod in activity fluctuations as observed during days without survey was disrupted during the sound exposure.

D. Potential range for masking problems

Assessing masking effects from seismic survey sound pulses for fishes or other aquatic animals is not an easy challenge (cf. Erbe *et al.*, 2016; Stanley *et al.*, 2017; Sills *et al.*, 2017; Pine *et al.*, 2020). Based on the acoustic tracking ability up to a distance of 18 km, we can conclude that the seismic pulses were sufficiently above ambient up to that distance to be detected, at least, by our equipment. This may

https://doi.org/10.1121/10.0006412

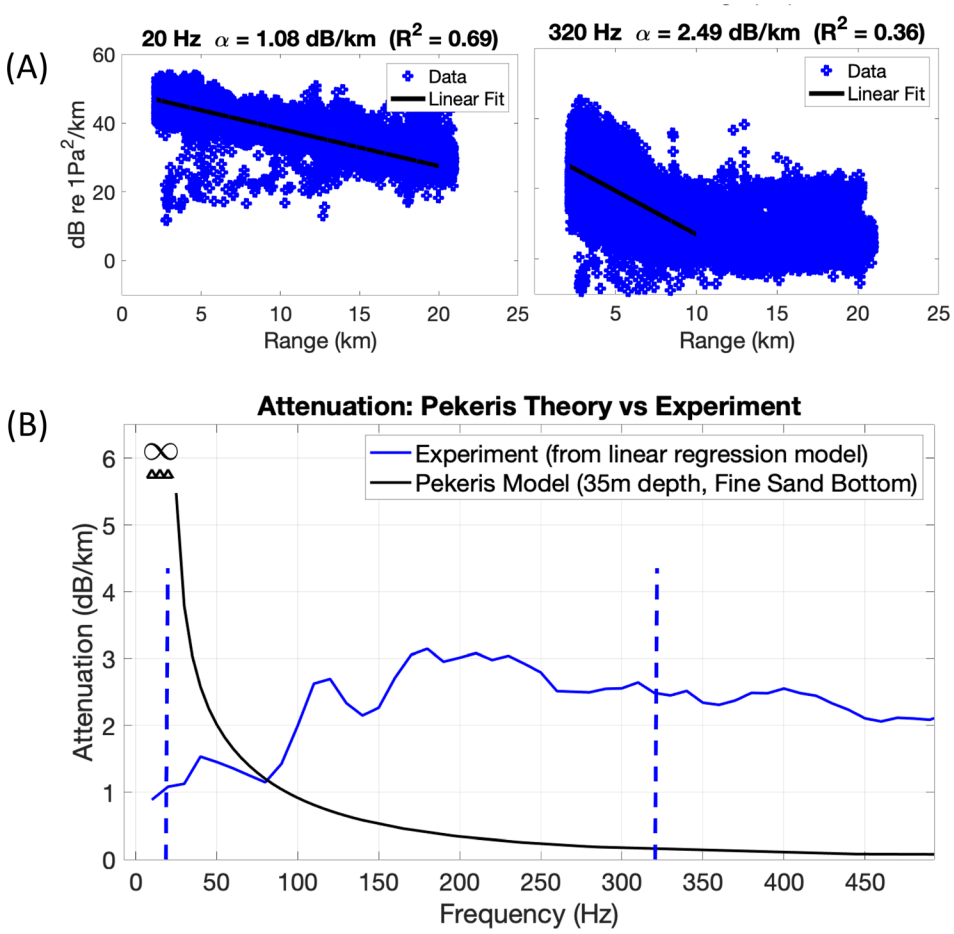

FIG. 9. (Color online) The frequency-dependent acoustic attenuation determined by the rms SPLs (10-s averaging time) of seismic pulse sounds with known propagation distance. (A) The blue circles show the rms pressure in dB for each seismic pulse as a function of the range for two different frequencies: 10 Hz on the left and 320 Hz on the right. The black lines are a linear fit to the data for each frequency. The slope of the line is the acoustic attenuation in dB/km. (B) The comparison of the experimental attenuation with a simple Pekeris model, which is a normal mode model for an iso-velocity shallow-water duct with a sediment bottom (in this case, 35 m depth and a fine sand bottom). The Pekeris model predicts the attenuation values, which are much higher at low frequencies and lower at high frequencies than the observed propagation data.

mean that the seismic pulses may also contribute to masking biologically relevant sound to fishes up to that distance from the vessel (see, e.g., Hawkins and Chapman, 1975; Vasconcelos *et al.*, 2007; Codarin *et al.*, 2009). The directionality cues available to us and the fish depend on the local particle acceleration patterns and also on the pressure fluctuations, which are both required to calculate the intensity. Fish may, therefore, rely on detection of each aspect to also use the combination of the sound aspects, like us, to determine the direction of the sound sources. The coherence between the pressure and particle velocity can also be used to extract the particle motion from the ambient noise (Rogers *et al.*, 2012), providing a perceptual strategy against masking, which is known as directional unmasking (Chapman, 1973; Chapman and Hawkins, 1973; Chapman and Johnstone, 1974), especially available to fish that can resolve the 180° directional ambiguity (see, e.g., Buwalda *et al.*, 1982).

An analysis of the signal-to-noise ratios for particle motion indicated that the seismic pulse was above the ambient level for only about 10 km. However, this may be an underestimate either due to the apparent sensitivity fading or inherent self-noise floor of our accelerometers. If we compare sound levels of the ambient noise at relatively quiet neap tide and noisy spring tide with the soundscape modifications during the survey, the sound pulses elevated the ambient levels up to 28 and 21 km, respectively. Masking may be avoided by so-called dip-listening in the periods between the subsequent pulses (Brumm and Slabbekoorn, 2005; Dooling and Leek, 2018), although sound levels were also above ambient for the intervals up to 21 km for sound pressure and up to about 1 km for particle motion.

For all of our discussion about auditory perception and masking, we should be aware that we typically lack sufficient insight into the critical ratios and critical bandwidths of the auditory filters for almost all species (Sand and Karlsen, 1986; Schuijf, 1975; Schuijf and Hawkins, 1983). Insights into the perceptual processing related to these phenomena may alter our understanding of the thresholds for detection and extraction of an acoustic signal from a particular background (Brumm and Slabbekoorn, 2005; Erbe *et al.*, 2016; Dooling and Leek, 2018) and, therefore, modulate the range of masking and possible disturbance. However, we hope our data and discussion will stimulate interest and trigger future studies.

V. CONCLUSION

We found distinct amplitude fluctuations matching the temporal pattern of the tidal currents in both the pressure and particle motion. We also found directionality patterns that were different for high and low tide currents and distinct and most prominent in the 10–20 Hz and 20–40 Hz frequency bands. We believe that these repeatable directional patterns are reported here for the first time and are most

likely caused by a relatively long-distance source of tidal currents associated with large rivers. The sounds of the experimental seismic survey were above the ambient conditions for our accelerometers up to 10 km from the source, and for pressures up to 31 km, which was the maximum distance of exposure during our study. The natural and anthropogenic noise patterns that we report here provide a novel perspective on the auditory world of fishes. They cause a shift in our understanding about potential ranges over which fishes may have access to acoustic cues for distant localities and could be affected by anthropogenic noise through masking and disturbance.

ACKNOWLEDGMENTS

This project was funded by the E and P Sound and Marine Life Joint Industry Programme (JIP). We thank Michael Ainslie for advice all along the trajectory of this project and for critical feedback on the manuscript and James Martin for many useful insights from his input during practical exercises and theoretical discussions. We thank all of the people that helped us with the deployment and recovery operations at sea, the research vessel (RV) Simon Stevin and the scientific diving team, provided by Vlaams Instituut voor de Zee (VLIZ) as part of the Flemish contribution to LifeWatch. Also, special thanks to the people from CGG, who were an excellent and professional partner at sea. The sea surface state dataset was provided by the Royal Belgian Institute of Natural Sciences, Directorate Natural Environment, Marine Forecasting Centre. Also, many thanks to the people from the Belgian (RBINS; Belgian Department of BPN) and Dutch authorities (MINEZ; RWS), who gave their critical support for getting the right permits to conduct the experimental seismic survey.

[1]See https://odnature.naturalsciences.be/marine-forecasting-centre/en/forecasts (Last viewed 11/11/2020).

Ahonen, H., Stafford, K. M., Steur, L., Lydersen, C., Wiig, Ø., and Kovacs, K. M. (**2017**). "The underwater soundscape in western Fram Strait: Breeding ground of Spitsbergen's endangered bowhead whales," Mar. Pollut. Bull. **123**, 97–112.

Amorim, M. C. P., Vasconcelos, R. O., and Fonseca, P. J. (**2015**). *Fish Sounds and Mate Choice. Sound Communication in Fishes*" (Springer, Berlin), pp 1–33.

Au, W. W. L. (**1993**). *The Sonar of Dolphins* (Springer-Verlag, New York).

Brabant, R., Degraer, S., and Rumes, B. (**2013**). "Monitoring offshore wind farms in the belgian part of the North sea: Setting the scene," in *Environmental Impacts of Offshore Wind Farms in the Belgian Part of the North Sea - Learning from the past to Optimise Future Monitoring Programmes*, edited by S. Degraer, R. Brabant, and B. Rumes (Royal Belgian Institute of Natural Sciences, Brussels), pp. 14–23.

Bruce, B., Bradford, R., Foster, S., Lee, K., Lansdell, M., Cooper, S., and Przeslawski, R. (**2018**). "Quantifying fish behaviour and commercial catch rates in relation to a marine seismic survey," Mar. Environ. Res. **140**, 18–30.

Brumm, H., and Slabbekoorn, H. (**2005**). "Acoustic communication in noise," Adv. Study Behavior **35**, 151–209.

Buwalda, R. J. A., Schuijf, A., and Hawkins, A. D. (**1982**). "Discrimination by the cod of sounds from opposing directions," J. Comp. Pysiol. **50**, 175–184.

Carroll, A. G., Przeslawski, R., Duncan, A., Gunning, M., and Bruce, B. (**2017**). "A critical review of the potential impacts of marine seismic surveys on fish and invertebrates," Mar. Pollut. Bull. **114**, 9–24.

Chapman, C. J. (**1973**). "Field studies of hearing in teleost fish," Helgoländer wiss. Meeresunters. **24**, 371–390.

Chapman, C. J., and Hawkins, A. D. (**1973**). "A field study of hearing in the cod, Gadus morhua L," J. Comp. Physiol. **85**, 147–167.

Chapman, C. J., and Johnstone, A. D. F. (**1974**). "Some auditory discrimination experiments on marine fish," J. Exp. Biol. **61**, 521–528.

Codarin, A., Wysocki, L. E., Ladich, F., and Picciulin, M. (**2009**). "Effects of ambient and boat noise on hearing and communication in three fish species living in a marine protected area (Miramare, Italy)," Mar. Pollut. Bull. **58**, 1880–1887.

Coquereau, L., Lossent, J., Grall, J., and Chauvaud, L. (**2017**). "Marine soundscape shaped by fishing activity," R. Soc. Open Sci. **4**, 160606.

Cox, H. (**1973**). "Spatial correlation in arbitrary noise fields with application to ambient sea noise," J. Acoust. Soc. Am. **54**, 1289–1301.

Cox, K., Brennan, L. P., Gerwing, T. G., Dudas, S. E., and Juanes, F. (**2018**). "Sound the alarm: A meta-analysis on the effect of aquatic noise on fish behavior and physiology," Glob. Change Biol. **24**, 3105–3116.

Crighton, D. G. (**1975**). "Basic principles of aerodynamic noise generation," Prog. Aerosp. Sci. **16**, 31–96.

Davidsen, J. G., Dong, H., Linne, M., Andersson, M. H., Piper, A., Prystay, T. S., Hvam, E. B., Thorstad, E. B., Whoriskey, F., and Cooke, S. J. (**2019**). "Effects of sound exposure from a seismic airgun on heart rate, acceleration and depth use in free-swimming Atlantic cod and saithe," Conserv. Physiol. **7**, 1–19.

Degraer, S., Brabant, R., Rumes, B., and Vigin, L. (eds.). (**2019**). *Environmental Impacts of Offshore Wind Farms in the Belgian Part of the North Sea: Marking a Decade of Monitoring, Research and Innovation* (Royal Belgian Institute of Natural Sciences, OD Natural Environment, Marine Ecology and Management, Brussels), 134 pp.

Dooling, R. J., and Leek, M. R. (**2018**). "Communication masking by man-made noise," in *Effects of Anthropogenic Noise on Animals. Springer Handbook of Auditory Research 66*, edited by H. Slabbekoorn, R. J. Dooling, A. N. Popper, and R. R. Fay (Springer, New York), pp. 23-46.

D'Spain, G. L., Luby, J. C., Wilson, G. R., and Gramann, R. A. (**2006**). "Vector sensors and vector sensor line arrays: Comments on optimal array gain and detection," J. Acoust. Soc. Am. **120**, 171–185.

Duarte, C. M., Chapuis, L., Collin, S. P., Costa, D. P., Devassy, R. P., Eguiluz, V. M., Erbe, C., Halpern, B. S., Harding, H., Havlik, M. N., Gordon, T. A. C., Merchant, N. D., Meekan, M., Miksis-Olds, J. L., Parsons, M., Predragovic, M., Radford, A. N., Radford, C. A., Simpson, S. D., Slabbekoorn, H., Staaterman, E., Van Opzeeland, I. C., Winderen, J., Zhang, X., and Juanes, F. (**2021**). "The soundscape of the Anthropocene ocean," Science **371**, eaba4658.

Duennebier, F. K., Lukas, R., Nosal, E.-M., Aucan, J., and Weller, R. A. (**2012**). "Wind, waves, and acoustic background levels at Station ALOHA," J. Geophys. Res. **117**, C03017, https://doi.org/10.1029/2011JC007267.

Engelmann, J., Hanke, W., Mogdans, J., and Bleckmann, H. (**2000**). "Neurobiology: Hydrodynamic stimuli and the fish lateral line," Nature **408**, 51–52.

Erbe, C., Reichmuth, C., Cunningham, K., Lucke, K., and Dooling, R. J. (**2016**). "Communication masking in marine mammals: A review and research strategy," Mar. Poll. Bull. **103**, 15–38.

Erisman, B. E., and Rowell, T. J. (**2017**). "A sound worth saving: Acoustic characteristics of a massive fish spawning aggregation," Biol. Lett. **13**, 20170656.

Estabrook, B. J., Ponirakis, D. W., Clark, C. W., and Rice, A. N. (**2016**). "Widespread spatial and temporal extent of anthropogenic noise across the northeastern Gulf of Mexico shelf ecosystem," Endang. Spec. Res. **30**, 267–282.

Fay, R. R. (**2009**). "Soundscapes and the sense of hearing of fishes," Int. Zool. **4**, 26–32.

Fewtrell, J. L., and McCauley, R. D. (**2012**). "Impact of air gun noise on the behaviour of marine fish and squid," Mar. Poll. Bull. **64**, 984–993.

Fine, M. L., and Parmentier, E. (**2015**). "Mechanisms of fish sound production," in *Sound Communication in Fishes, Animal Signals and Communication*, edited by F. Ladich (Springer, Berlin), Vol. 4, pp 77–126.

Fried, S. E., Walker, S. C., Hodgkiss, W. S., and Kuperman, W. A. (**2013**). "Measuring the effect of ambient noise directionality and split-beam processing on the convergence of the cross-correlation function," J. Acoust. Soc. Am. **134**, 1824–1832.
Frisk, G. V. (**2012**). "Noiseonomics: The relationship between ambient noise levels in the sea and global economic trends," Sci. Rep. **2**, 437.
Gannon, D. P., Barros, N. B., Nowacek, D. P., Read, A. J., Waples, D. M., and Wells, R. S. (**2005**). "Prey detection by bottlenose dolphins, *Tursiops truncatus*: An experimental test of the passive listening hypothesis," Anim. Behav. **69**, 709–720.
Gisiner, R. C. (**2016**). "Sound and marine seismic surveys," Acoust. Today **12**, 10–18.
Greene, C. R., McLennan, M. W., Norman, R. G., McDonald, T. L., Jakubczak, R. S., and Richardson, W. J. (**2004**). "Directional frequency and recording (DIFAR) sensors in seafloor recorders to locate calling bowhead whales during their fall migration," J. Acoust. Soc. Am. **116**, 799–813.
Halliday, W. D., Pine, M. K., Bose, A. P. H., Balshine, S., and Juanes, F. (**2018**). "The plainfin midshipman's soundscape at two sites around Vancouver Island, British Columbia," Mar. Ecol. Progr. Ser. **603**, 189–200.
Hassel, A., Knutsen, T., Dalen, J., Skaar, K., Løkkeborg, S., Misund, O. A., Østensen, Ø., Fonn, M., and Haugland, E. K. (**2004**). "Influence of seismic shooting on the lesser sandeel (*Ammodytes marinus*)," ICES J. Mar. Sci. **61**, 1165–1173.
Hawkins, A. D., and Chapman, C. J. (**1975**). "Masked auditory thresholds in the cod, *Gadus morhua* L.," J. Comp. Physiol. A **103**, 209–226.
Hawkins, A. D., Pembroke, A. E., and Popper, A. N. (**2015**). "Information gaps in understanding the effects of noise on fishes and invertebrates," Rev. Fish Biol. Fish. **25**, 39–64.
Hazelwood, R. A. (**2012**). "Ground roll waves as a potential influence on fish: Measurements and analysis techniques," Adv. Exp. Med. Biol. **730**, 449–452.
Hildebrand, J. A. (**2009**). "Anthropogenic and natural sources of ambient noise in the ocean," Mar. Ecol. Progr. Ser. **395**, 5–20.
Howe, B. M., Miksis-Olds, J., Rehm, E., Sagen, H., Worcester, P. F., and Haralabus, G. (**2019**). "Observing the oceans acoustically," Front. Mar. Sci. **6**, 1–22.
Hubert, J., Campbell, J. A., and Slabbekoorn, H. (**2020**). "Effects of seismic airgun playbacks on swimming patterns and behavioural states of Atlantic cod in a net pen," Mar. Poll. Bull. **160**, 111680.
Jensen, F. B., Kuperman, W. A., Porter, M. B., and Schmidt, H. (**2011**). *Computational Ocean Acoustics* (Springer, New York).
Kennedy, E. V., Guzman, H. M., Holderied, M. W., Mair, J. M., and Simpson, S. D. (**2010**). "Reef generated noise provides reliable information about habitats and communities: Evidence from a Panamanian case study," J. Exp. Mar. Biol. Ecol. **395**, 85–92.
Kok, A. C. M., Bruil, L., Berges, B., Sakinan, S., Debusschere, E., Reubens, J., de Haan, D., Norro, A., and Slabbekoorn, H. (**2021**). "An echosounder view on the potential effects of impulsive noise pollution on pelagic fish around windfarms in the North Sea," Environ. Poll. **290**, 118063.
Kunc, H. P., McLaughlin, K. E., and Schmidt, R. (**2016**). "Aquatic noise pollution: Implications for individuals, populations, and ecosystems," Proc. R. Soc. London B **283**, 20160839.
Ladich, F. (**2008**). "Sound communication in fishes and the influence of ambient and anthropogenic noise," Bioacoustics **17**, 34–38.
Ladich, F., and Fay, R. R. (**2013**). "Auditory evoked potential audiometry in fish," Rev. Fish Biol. Fish. **23**, 317–364.
Larsen, O. N., and Radford, C. (**2018**). "Acoustic conditions affecting sound communication in air and underwater," in *Effects of Anthropogenic Noise on Animals. Springer Handbook of Auditory Research*, edited by H. Slabbekoorn, R. J. Dooling, A. N. Popper, and R. R. Fay (Springer, New York), Vol. 66, pp. 109–144.
Lillis, A., and Mooney, T. A. (**2018**). "Snapping shrimp sound production patterns on Caribbean coral reefs: Relationships with celestial cycles and environmental variables," Cor. Reefs **37**, 597–607.
Longuet-Higgins, M. S. (**1950**). "A theory on the origin of microseisms," Phil. Trans. Roy. Soc. London Ser. A **243**, 1–35.
Martin, S. B., Morris, C., Bröker, K., and O'Neill, C. (**2019**). "Sound exposure level as a metric for analyzing and managing underwater soundscapes," J. Acoust. Soc. Am. **146**, 135–149.
McCreery, C. S., Sutton, G. H., and Duennebier, F. K. (**1993**). "Correlation of deep ocean noise (0.4–30 Hz) with wind, and the Holu Spectrum—A worldwide constant," J. Acoust. Soc. Am. **93**, 2639–2648.
McDonald, M. A., Hildebrand, J. A., and Wiggins, S. M. (**2006**). "Increases in deep ocean ambient noise in the Northeast Pacific west of San Nicolas Island, California," J. Acoust. Soc. Am. **120**, 711–718.
McWilliam, J. N., and Hawkins, A. D. (**2013**). "A comparison of inshore marine soundscapes," J. Exp. Mar. Biol. Ecol. **446**, 166–176.
Miksis-Olds, J. L., Martin, B., and Tyack, P. L. (**2018**). "Exploring the ocean through soundscapes," Acoust. Today **14**, 26–34.
Morris, C. J., Cote, D., Martin, B., and Kehler, D. (**2018**). "Effects of 2D seismic on the snow crabfishery," Fisheries Res. **197**, 67–77.
Morris, C. J., Cote, D., Martin, B., and Mullowney, D. (**2020**). "Effects of 3D seismic surveying on snow crabfishery," Fisheries Res. **232**, 105719.
Nedelec, S., Campbell, J. A., Radford, A., Simpson, S., and Merchant, N. (**2016**). "Particle motion: The missing link in underwater acoustic ecology," Meth. Ecol. Evol. **7**, 836–842.
Nichols, R. H., and Sayer, C. E. (**1977**). "Frequency-frequency correlations of ocean ambient noise levels," J. Acoust. Soc. Am. **61**, 1188–1190.
Nichols, S. M., and Bradley, D. L. (**2019**). "Use of noise correlation matrices to interpret ocean ambient noise," J. Acoust. Soc. Am. **145**, 2337–2349.
Nilsson, H., Van Overloop, J., Mehdi, R. A., and Pålsson, J. (**2017**). "Transnational maritime spatial planning in the North Sea: The Shipping Context Report on Work-package 4 of the NorthSEE Project," 55 pp.
Pearson, W. H., Skalski, J. R., and Malme, C. I. (**1992**). "Effects of sounds from a geophysical survey device on behavior of captive rockfish (*Sebastes* spp.)," Can. J. Fish. Aquat. Sci. **49**, 1343–1356.
Pekeris, C. L. (**1948**). "Theory of propagation of explosive sound in shallow water," Mem.-Geol. Soc. Am. **27**, 1–117.
Pine, M. K., Nikolich, K., Martin, B., Morris, C., and Juanes, F. (**2020**). "Assessing auditory masking for management of underwater anthropogenic noise," J. Acoust. Soc. Am. **147**, 2337–2349.
Popper, A. N., and Fay, R. R. (**2011**). "Rethinking sound detection by fishes," Hear. Res. **273**, 25–36.
Popper, A. N., and Hawkins, A. D. (**2018**). "The importance of particle motion to fishes and invertebrates," J. Acoust. Soc. Am. **143**, 470–488.
Popper, A. N., and Hawkins, A. D. (**2019**). "An overview of fish bioacoustics and the impacts of anthropogenic sounds on fishes," J. Fish. Biol. **94**, 692–713.
Popper, A. N., Hawkins, A. D., Fay, R. R., Mann, D. A., Bartol, S., Carlson, T. J., and Halvorsen, M. B. (**2014**). "ASA S3/SC1.4 TR-2014 Sound Exposure Guidelines for Fishes and Sea Turtles," in *Springer Briefs in Oceanography, A Technical Report Prepared by ANSI-Accredited Standards Committee S3/SC1 and Registered with ANSI* (Springer, Cham).
Prosperetti, A. (**1988**). "Bubble dynamics in oceanic ambient noise," in *Sea Surface Sound. NATO ASI Series (Series C: Mathematical and Physical Sciences)*, edited by B. R. Kerman (Springer, Dordrecht), Vol. 238.
Radford, C. A., Jeffs, A. G., Tindle, C. T., and Montgomery, J. C. (**2008**). "Temporal patterns in ambient noise of biological origin from a shallow water temperate reef," Behav. Ecol. **156**, 921–929.
Radford, C. A., Stanley, J. A., Hole, W., Montgomery, J. C., and Jeffs, A. (**2010**). "Localised coastal habitats have distinct underwater sound signatures," Mar. Ecol. Progr. Ser. **401**, 21–29.
Roberts, L., and Elliot, M. (**2017**). "Good or bad vibrations? Impacts of anthropogenic vibration on the marine epibethos," Sci. Total Environ. **595**, 255–268.
Rogers, P. H., Martin, J. S., and Bogle, J. R. (**2012**). "A critical reevaluation of the role of acoustic pressure in source localization by fish," in *The Effects of Noise on Aquatic Life. Advances in Experimental Medicine and Biology*, edited by A. N. Popper and A. Hawkins (Springer, New York), Vol. 730.
Sand, O., and Karlsen, H. E. (**1986**). "Detection of infrasound by the Atlantic cod," J. Exp. Biol. **125**, 197–204.
Schuijf, A. (**1975**). "Directional hearing of cod (*Gadus morhua*) under approximate free field conditions," J. Comp. Physiol. **98**, 307–332.
Schuijf, A., and Hawkins, A. D. (**1983**). "Acoustic distance discrimination by the cod," Nature **302**, 143–144.
Sertlek, H. Ö., Slabbekoorn, H., ten Cate, C., and Ainslie, M. A. (**2019**). "Source specific sound mapping: Spatial, temporal and spectral distribution of sound in the Dutch North Sea," Environm. Poll. **247**, 1143–1157.

Sills, J. M., Southall, B. L., and Reichmuth, C. (**2017**). "The influence of temporally varying noise from seismic air guns on the detection of underwater sounds by seals," J. Acoust. Soc. Am. **141**, 996–1008.
Simpson, S. D., Meekan, M., Montgomery, J., McCauley, R., and Jeffs, A. (**2005**). "Homeward sound," Science **308**, 221.
Slabbekoorn, H., and Bouton, N. (**2008**). "Soundscape orientation: A new field in need of sound investigation," Anim. Behav. **76**, e5–e8.
Slabbekoorn, H., Bouton, N., van Opzeeland, I., Coers, A., ten Cate, C., and Popper, A. N. (**2010**). "A noisy spring: The impact of globally rising underwater sound levels on fish," Trends Ecol. Evol. **25**, 419–427.
Slabbekoorn, H., Dalen, J., de Haan, D., Winter, H. V., Radford, C., Ainslie, M. A., Heaney, K. D., van Kooten, T., Thomas, L., and Harwood, J. (**2019**). "Population-level consequences of seismic surveys on fishes: An interdisciplinary challenge," Fish Fish. **20**, 653–685.
Slabbekoorn, H., Dooling, R. J., Popper, A. N., and Fay, R. R. (**2018**). "Effects of anthropogenic noise on animals," in *Springer Handbook of Auditory Research* (Springer, New York), Vol. 66.
Soudijn, F. H., van Kooten, T., Slabbekoorn, H., and de Roos, A. M. (**2020**). "Population-level effects of acoustic disturbance in Atlantic cod: A size-structured analysis based on energy budgets," Proc. R. Soc. B Biol. Sci. **287**, 20200490.
Southall, B. L., Finneran, J. J., Reichmuth, C., Nachtigall, P. E., Ketten, D. R., Bowles, A. E., Ellison, W. T., Nowacek, D. P., and Tyack, P. L. (**2019**). "Marine mammal noise exposure criteria: Updated scientific recommendations for residual hearing effects," Aquat. Mamm. **45**, 125–232.
Staaterman, E., Rice, A. N., Mann, D. A., and Paris, C. B. (**2013**). "Soundscapes from a tropical eastern Pacific reef and a Caribbean sea reef," Cor. Reefs **32**, 553–557.
Stanley, J. A., Van Parijs, S. M., and Hatch, L. T. (**2017**). "Underwater sound from vessel traffic reduces the effective communication range in Atlantic cod and haddock," Sci. Rep. **7**, 14633.
Strobel, M., and Mooney, T. A. (**2012**). "Detection of low-frequency tones and whale predatorsounds by the American sand lance *Ammodytes americanus*," J. Fish Biol. **81**, 1646–1664.
Thode, A. M., Blackwell, S. B., Conrad, A. S., and Kim, K. H. (**2017**). "Long-term measurements of the ice-free underwater noise field directionality in the shallow Beaufort Sea," J. Acoust. Soc. Am. **142**, 2486.
Thode, A. M., D'Spain, G. L., and Kuperman, W. A. (**2000**). "Matched-field processing and geoacoustic inversion of blue whale vocalizations," J. Acoust. Soc. Am. **107**, 1286–1300.
Thode, A. M., Sakai, T., Michalec, J., Rankin, S., Soldevilla, M. S., Martin, B., and Kim, K. H. (**2019**). "Displaying bioacoustic directional information from sonobuoys using 'azigrams,'" J. Acoust. Soc. Am. **146**, 95–102.
Tolstoy, M., Bohnenstiehl, D. R., and Chapp, E. (**2004**). "Long range acoustic propagation of high frequency energy in the Indian Ocean from icebergs and earthquakes," in *Proc. of the 26th Seismic Research Review: Trends in Nuclear Explosion Monitoring*, Orlando, FL, pp. 519–534.
Urick, R. J. (**1975**). *Principles of Underwater Sound* (McGraw-Hill, New York).
Van der Knaap, I., Reubens, J., Ainslie, M., Thomas, L., Winter, H. V., Hubert, J., Martin, B., and Slabbekoorn, H. (**2021b**). "Effects of a seismic survey on movement of free-ranging Atlantic cod," Curr. Biol. **31**, 1555–1562.
Van der Knaap, I., Slabbekoorn, H., Winter, H. V., Moens, T., and Reubens, J. (**2021**). "Evaluating receiver contributions to Acoustic Positional Telemetry: A case study on Atlantic cod around wind turbines in the North Sea," Anim. Biotel. **9**, 14.
Vasconcelos, R. O., Amorim, M. C. P., and Ladich, F. (**2007**). "Effects of ship noise on the detectability of communication signals in the Lusitanian toadfish," J. Exp. Biol. **210**, 2104–2112.
Walker, S. C., and Buckingham, M. J. (**2012**). "Spatial coherence and cross correlation of three-dimensional ambient noise fields in the ocean," J. Acoust. Soc. Am. **131**, 1079–1086.
Wenz, G. M. (**1962**). "Acoustic ambient noise in the ocean: Spectra and sources," J. Acoust. Soc. Am. **34**, 1936–1956.
Wilson, O., Jr., Wolf, S. N., and Ingenito, F. (**1985**). "Measurements of acoustic ambient noise in shallow water due to breaking surf," J. Acoust. Soc. Am. **78**, 190–195.
Yang, Q., Yang, K., Cao, R., and Duan, S. (**2018**). "Spatial vertical directionality and correlation of low-frequency ambient noise in deep ocean direct-arrival zones," Sensors **18**, 319.
Zhou, J. (**2020**). "Analysis of ambient noise spectrum level correlation characteristics in the China Sea," IEEE Acces **8**, 7217–7226.